Scientific Reports

https://doi.org/10.1038/s41598-025-34826-2

Article in Press

Streamlined rAAV HeLaS3 producer cell line generation via *GS* selection

Received: 10 October 2025

Accepted: 31 December 2025

Published online: 09 January 2026

Cite this article as: Antunes M., Moura F., Sebastian I.R. *et al.* Streamlined rAAV HeLaS3 producer cell line generation via *GS* selection. *Sci Rep* (2026). https://doi.org/10.1038/s41598-025-34826-2

Mariana Antunes, Filipa Moura, Ivy Rose Sebastian, Paula Alves, Patrícia Gomes-Alves & Jose M. Escandell

Streamlined rAAV HeLaS3 Producer Cell Line Generation via *GS* Selection

Mariana Antunes[1,2], Filipa Moura[1,2], Ivy Rose Sebastian[3], Paula Alves[1,2], Patrícia Gomes-Alves[1,2], Jose M Escandell[1,2,†]

[1]*iBET, Instituto de Biologia Experimental e Tecnológica, Apartado 12, 2781-901 Oeiras, Portugal*
[2]*Instituto de Tecnologia Química e Biológica António Xavier, Universidade Nova de Lisboa, Av. da República, 2780-157 Oeiras, Portugal*
[3] *BOKU University, Institute of Animal Cell Technology and Systems Biology, Department of Biotechnology and Food Science, Muthgasse 11, 1190 Vienna, Austria*

[†]Corresponding author

Keywords: Glutamine synthetase (*GLUL*), rAAV production, HeLaS3 cell line, Producer cell line (PCL), Gene therapy manufacturing

Abstract

The high cost and complexity of manufacturing recombinant adeno-associated virus vectors continue to limit the broader application of gene therapies, which offer life-changing potential for individuals affected by genetic diseases. Although stable producer cell lines represent a scalable and cost-effective alternative to transient transfection methods, their development is often delayed by inefficient selection strategies and extended timelines. In this study, we present a novel application of the glutamine synthetase-based selection system -commonly used in CHO cells- to a HeLaS3-based rAAV production platform. By generating glutamine synthetase-knockout HeLaS3 cells via CRISPR-Cas9 and applying glutamine deprivation under serum-free conditions, we significantly streamlined the PCL generation process, reducing the timeline to approximately two months while maintaining rAAV productivity (>$1x10^{11}$ vg/mL) and product quality (~70% full capsids). This work establishes a robust and scalable workflow for rAAV manufacturing, with the potential to enhance accessibility and reduce viral vector production costs for applications in gene therapy.

Introduction

Recombinant adeno-associated virus (rAAV)-based vectors have become widely used in gene therapy, serving as efficient vehicles for in vivo delivery of therapeutic genes. They combine low pathogenicity and low toxicity with broad cell tropism and the ability to support long-term gene expression, making them a versatile and safe platform for treating a wide range of genetic disorders[1]. However, while more than 300 clinical trials have been conducted and eight rAAV-based therapies have been approved so far[2], some of these therapies have been withdrawn, and research efforts are currently being scaled back due to the high manufacturing costs[3]. These challenges highlight the urgent need to improve recombinant AAV production processes to reduce costs and ensure the continued advancement and accessibility of gene therapy.

Current manufacturing systems primarily rely on Human Embryonic Kidney (HEK) 293 transient transfection, which is the most straightforward and fast approach for rAAV production, offering flexibility during the early stages of product development[4]. However, while the transient transfection system offers advantages in terms of overall timelines and flexibility, it lacks robustness, limits product quality, and poses significant challenges for large-scale manufacturing—factors that contribute to elevated production costs[5]. On the other hand, producer cell lines (PCL) present a promising alternative, providing higher scalability, robustness, and product quality[4].

The HeLaS3 based PCL platform is a well-established and promising system for rAAV production. Originally developed by Clark et al. (1995)[6], this platform has undergone significant improvements to meet industrial standards and enhance regulatory compliance[7–9]. Despite these advancements, establishing a producer cell line remains time-intensive (typically 6–8 months) and requires a complex protocol involving dual screening stages, which continues to pose a major challenge[7–9].

This study introduces the adaptation of the glutamine synthetase (*GS*)-based selection system—widely used in Chinese Hamster Ovary (CHO) cells for monoclonal antibody production—to the HeLaS3 platform for the generation of rAAV producer cell lines. By integrating this selection strategy into a fully suspension-adapted, serum-free workflow, we establish a streamlined and scalable process that enables efficient cell line development and robust rAAV production. Furthermore, we demonstrate that combining *GS*-based selection with glutamine (Gln)-deprived conditions not only enables stringent selection of high-producing clones but also enhances rAAV productivity by reducing ammonia accumulation during production. Collectively, these results validate a versatile and scalable platform that addresses key limitations of current transient transfection-

based systems and supports the development of next-generation gene therapy manufacturing processes.

Results

Generation and Characterization of GLUL$^{-/-}$ HeLaS3 Cell Lines

Previous efforts to implement suspension-based selection using antibiotic resistance markers in HeLaS3 cells for rAAV production have largely been unsuccessful, often resulting in poor enrichment and limited cell viability[7,8]. To address this, we aimed to evaluate the applicability of the *GS*-based selection system under Gln-depleted, serum-free conditions. Originally developed for CHO cells, this approach has been also adapted for HEK293 cells, supporting not only monoclonal antibody[10] production but also the expression of various recombinant proteins[11]. To evaluate the suitability of *GS*-based selection systems for rAAV production, we generated a *GLUL*-knockout (the human homologous to *GS*) HeLaS3 cell line. In this selection system, cells become auxotrophic for Gln, and the gene of interest is co-expressed from a plasmid carrying the *GLUL* gene. Upon transfection, the plasmid integrates into the genome, and cells are selected under Gln-depleted conditions, allowing only those with successful integration to survive[12].

Figure 1A shows the structure of the human *GLUL* gene and its isoforms, highlighting exon 5, which encodes the catalytic domain. To disrupt *GLUL* expression in HeLaS3 cells, we performed CRISPR-Cas9 gene editing using a single guide RNA targeting exon 5. Cells were transfected via nucleofection with CRISPR-Cas9 ribonucleoprotein complexes. Editing efficiency was assessed three days post-transfection using a T7 endonuclease I assay, which indicated a cleavage rate of approximately 65% (Fig. 1B).

Clones were obtained from the transfected cell pool, through limiting cell dilution. Single cell cloning was confirmed by imaging at days 0, 3 and 10 after seeding (Fig.1C). Clones were amplified for further testing and to assess the efficiency of *GLUL* gene disruption, we performed Western blot analysis (Fig. 1D) on three CRISPR-edited HeLa clones (GKO1, GKO2, and GKO3). Interestingly, Clone GKO1 displayed a distinct migration pattern (lower MW band) compared to wild-type (WT) HeLaS3 cells, indicating the presence of a truncated GLUL protein. The sgRNA to delete *GLUL* gene was designed near the exon 5 splice site, leading us to hypothesize that the splicing site may be disrupted in this clone. Supporting this, nanopore sequencing analysis of Clone GKO1 (Suppl. Fig 1) revealed a subset of alignment sequences with large deletions in the splicing site region. Although the GLUL protein is still expressed in this clone, given that this exon encodes a critical region of the enzyme's active site[10], the resulting protein is

expected to be non-functional despite its expression. In contrast, clones GKO2 and GKO3 showed no detectable GLUL protein, consistent with complete knockout.

To assess functional Gln auxotrophy, HeLaS3 wild-type and *GLUL*$^{-/-}$ clones (GKO1 and GKO3) were analysed. Clone GKO2 was excluded from functional assays due to impaired cell growth, suggesting a potential off-target effect. In Gln-supplemented culture conditions, no differences in viability were observed between wild-type and *GLUL*$^{-/-}$ clones (Fig. 2A).

When HeLaS3 cells were cultured under glutamine-depleted conditions, a pronounced decline in cell viability was observed (Fig. 2B). After nine days, a clear distinction emerged between *GLUL*$^{-/-}$ clones and WT cells, with viability decreasing to 9% in GKO1 and 12% in GKO3, compared to 60% in WT cells. As expected, no differences were observed in Gln depleted conditions in clone GKO3 and GKO1, confirming that GKO1 truncated form of GLUL is not functional. Moreover, WT cells were able to adapt to growth in this serum-free medium, achieving lower and stable PDTs (~35 h) after subculturing cells for 42 days (Suppl. Fig. 2) due to overexpression of *GLUL* endogenous gene (Suppl. Fig. 3), which would increase the background of this selection methodology. This data suggests that the use of HeLaS3 *GLUL*$^{-/-}$ clones is required for the *GLUL* selection process.

_GS_-Based Selection and Enrichment of rAAV-Producing Cells

To assess the feasibility of selecting rAAV-producing clones directly in suspension culture and to streamline the generation of high-rAAV producing HeLaS3 lines, we transfected the *GLUL* knockout clone GKO1 with rAAV5 producing plasmid (Suppl. Fig 4). Selection was then carried out under glutamine-depleted, serum-free, suspension culture conditions (Fig. 3A). As expected, non-transfected control cells failed to expand under selective pressure (Fig. 3B), confirming the stringency of the Gln-deprived selection. In contrast, transfected cells showed recovery of viability and resumed proliferation by day 14 post-transfection (Fig. 3B), achieving 90 % of cell viability after 22 days indicating successful enrichment of transgene-expressing cells.

Following adaptation and enrichment, single-cell cloning was performed under serum-free conditions (Fig. 3A). Expanded clones were screened for rAAV5 productivity. As shown in Fig. 3C, a broad range of vector genome titers (vg/mL) was observed among individual clones, with several exceeding volumetric productivity of 10^{10} vg/mL. Cell specific production yield (qP, vg/cell) is presented in Fig. 3D, further confirming the identification of high-producing clones achieving a qP of 3×10^{5} vg/cell. These results

demonstrate that the suspension-based selection strategy is effective for isolating rAAV-producing HeLaS3 *GLUL*$^{-/-}$ clones with high productivity.

Characterization and Performance of the HeLaS3 *GS*-Based Platform

To validate the platform performance and characterize stable integration of the transgene, three high-producing clones were selected for scale-up and further analysis. As shown in Fig. 4A, rAAV5 volumetric productivity was confirmed in shake flask cultures, with Clone 1 showing vector genome titers exceeding 4×10^{10} vg/mL, consistent with initial screening results.

We next evaluated GLUL expression levels by Western blot analysis (Fig. 4B). Compared to the parental HeLaS3 *GLUL*$^{-/-}$ line (GKO1), the transfected pool and all selected clones expressed detectable GLUL protein, confirming functional rescue of GLUL under selective pressure triggered by plasmid integration.

To evaluate transgene stability and integration, we quantified rAAV cassette copy number by droplet digital PCR (ddPCR) (Fig. 4C). All analyzed clones carried multiple copies per genome, which correlated with their respective productivity levels (Fig. 4A). Clone 1 displayed the highest copy number (14.38 ± 0.56 copies/genome), consistent with its higher rAAV yield. These values are in line with those recently reported for a comparable platform based on *GLUL* wild-type cells and an alternative selection strategy[9].

Mass photometry of purified rAAV5 produced in PCL *GLUL*$^{-/-}$ cells (GKO1, 66 h post-infection) revealed two distinct populations, corresponding to molecular masses matching expected full and empty capsids (Fig. 4D). Full particles comprised ~70% of the total, confirming efficient genome packaging and platform robustness. Moreover, these purified vectors were also shown to be infective, as evidenced by the presence of GFP-positive cells following transduction (Suppl. Fig. 5).

This selection workflow was also validated with the rAAV2 serotype (Suppl. Fig. 6). The GKO1 clone was transfected with a plasmid encoding rAAV2 carrying GFP as the transgene (Suppl. Fig. 1) and selected under glutamine-depleted conditions. After pool recovery (Suppl. Fig. 6A), cells were seeded as single cells in serum-free conditions. Following single-cell outgrowth, clones were tested for rAAV production (Suppl. Fig. 6B), and the best-producing clones were successfully adapted to suspension culture, achieving titers above 10^{10} vg/mL (Suppl. Fig. 6C). This confirms the versatility and robustness of the approach across different serotypes. Moreover, the rAAV2 vectors generated using this GS$^{-/-}$ based platform demonstrated the ability to transduce cells, as shown in Suppl. Fig. 7.

As rAAV production does not occur in growth medium, the HeLaS3 platform requires separation of cell expansion and vector manufacturing into two distinct phases using dedicated media: a growth medium to support proliferation and a production medium to enable vector generation[7]. To evaluate the role of Gln in this selection system in both phases, we assessed its impact on cell growth and rAAV productivity under supplemented and deprived conditions. In growth medium, cells cultured without Gln exhibited a population doubling time of 35 ± 0.6 h, whereas Gln supplementation significantly enhanced proliferation, reducing doubling time to 26 ± 0.7 h (Fig. 5A). Accordingly, Gln-supplemented medium was used for cell expansion and subsequent experiments.

Next, we tested rAAV productivity in Gln-deprived and supplemented media. Notably, rAAV5 production was markedly higher under Gln-depleted conditions, yielding an almost three-fold increase in volumetric productivity compared to Gln-supplemented cultures ($1.3\times10^{11} \pm 0.4\times10^{11}$ vg/mL vs. $0.5\times10^{11} \pm 0.09\times10^{11}$ vg/mL; Fig. 5B). qP was also enhanced, reaching $2.1\times10^{5} \pm 0.4\times10^{5}$ vg/cell in Gln-deprived conditions versus $0.7\times10^{5} \pm 0.1\times10^{5}$ vg/cell with Gln. Moreover, ammonia (NH_3) accumulation, a byproduct of Gln metabolism, was substantially reduced in Gln-deprived cultures (0.17 ± 0.05 mM vs. 2.19 ± 0.37 mM in Gln-supplemented conditions; Fig. 5C), with negligible production rates in Gln-depleted conditions (-0.0022 ± 0.0019 mM/10^6 cells·h^{-1} vs. 0.0511 ± 0.0042 mM/10^6 cells·h^{-1}; Fig. 5D). These findings suggest that reduced ammonia accumulation contributes to enhanced rAAV productivity under Gln-deprived conditions.

Discussion

The manufacturing of recombinant rAAV vectors remains a critical bottleneck in gene therapy development, primarily due to high production costs and the limited scalability of transient transfection methods currently used for production. Although transient transfection in HEK293 cells dominates industrial practice, its dependence on GMP-grade plasmids and susceptibility to batch-to-batch variability significantly increases cost and complexity. In contrast, stable producer cell lines offer a promising alternative, providing improved scalability and cost-effectiveness. However, their widespread adoption has been hindered by extended development timelines, which remain a major barrier to establishing this approach as a viable solution for the future of gene therapy[4,13].

In this study, we adapted the *GS*-based selection system - widely used in CHO cell platforms for monoclonal antibody production - for the HeLaS3-based rAAV production platform. HeLaS3 based production platform were selected for this study due to its robustness and recent advances in upstream and downstream processing[7,14]. The

approach here presented addresses a key limitation of traditional dual-selection workflows used in the HeLaS3 platform, which typically require 6–8 months for PCL generation[7,8]. By enabling direct selection and single-cell cloning in suspension cultures, this approach reduced the timeline to approximately two months, aligning with industry efforts to accelerate cell line development.

A critical factor in *GS*-based selection is the Gln metabolism. Consistent with previous reports, Gln deprivation initially caused growth arrest and viability loss in wild-type HeLaS3 cells[15,16]. However, adaptation via upregulation of endogenous GLUL compromised selection stringency, necessitating *GLUL* knockout to enforce Gln auxotrophy (Suppl. Fig. 2 and Suppl. Fig. 3). This strategy mirrors previous findings in HEK293 and CHO systems, where *GS* knockout significantly improved selection efficiency[10,17]. Our *GLUL* knockout clones exhibited strict Gln dependence, validating their suitability as host cells for rAAV production.

Following selection, engineered cells expressing exogenous *GLUL* and rAAV components achieved high titers (>10^{11} vg/mL) under serum-free suspension conditions. Notably, while Gln-free media were essential during selection, supplementation post-selection improved cell growth and viability, pointing to a limitation in the ability to produce enough Gln for cell's metabolic needs. Interestingly, during the production phase, Gln-free conditions enhanced rAAV yields. We hypothesize that (1) reduced ammonia accumulation - known to negatively impact rAAV quality at concentrations >1 mM[14] - and (2) potential transcriptional coupling between *GLUL* and rAAV genes may contribute to this effect, possibly enhancing Rep gene amplification[8].

This platform consistently delivers high-quality rAAV particles with approximately 70% full capsids, significantly outperforming conventional transient transfection-based production systems, which typically achieve only 10–30% full capsids depending on the serotype[4]. This elevated proportion of full particles not only enhances overall product quality but also represents a substantial advantage for DSP; higher full-to-empty ratios reduce the burden on purification steps, improve process efficiency, and facilitate compliance with stringent regulatory expectations for product consistency and potency. Furthermore, its applicability to different serotypes (rAAV2 and rAAV5) underscores its versatility. These results align with recent reports advocating for stable cell line platforms as a scalable alternative to transient systems, which remain constrained by cost and variability[18,19].

In conclusion, this *GS*-based selection strategy significantly accelerates PCL development, reducing current timelines from 6–8 months to approximately 2 months,

while delivering high titers and enhanced product quality. Historically, key opinion leaders in the gene therapy field have faced a strategic dilemma at project inception: whether to rely on transient transfection for speed or invest in generating a PCL for long-term scalability and cost efficiency. Too often, the transient route is selected for rapid entry into clinical trials, only to encounter a manufacturing bottleneck in late-stage development—where capacity constraints, variability, and DSP challenges jeopardize readiness for process performance qualification and biologics license application submissions[19–21]. At that stage, pivoting to a PCL is typically impractical because it triggers major chemistry, manufacturing, and controls (CMC) changes, comparability risks, and timeline resets. By compressing PCL generation to ~2 months without compromising quality, our approach resolves this conundrum: enabling early adoption of stable PCLs, de-risking late-stage manufacturing, streamlining DSP with higher full capsid content, and maintaining a seamless path to pivotal supply and commercialization.

Future work will focus on optimizing upstream processes of this *GS*-based platform by leveraging knowledge from established CHO cell processes and *GS*-based selection systems implemented for other biologics production platforms. This includes media or feed optimization to enhance productivity and robustness. Additionally, efforts will be directed at expanding the platform to different serotypes and therapeutic cargos, while ensuring the integrity of the packaged rAAV genome and confirming the absence of host-related impurities (possible co-packaged). Finally, the platform will be scaled to perfusion bioreactors to enable continuous manufacturing—an approach increasingly recognized as critical for meeting clinical demand[19].

Materials and Methods

Cell culture

HeLaS3 cell line was acquired from ATCC (CCL-2.2) and maintained in adherent culture at 37 ºC and in a 5 % CO_2 atmosphere, in Dulbecco's Modified Eagle's Medium (DMEM) (10-013-CV, Corning) supplemented with 10 % Fetal Bovine Serum (FBS) (1027016, Gibco). Cells were subcultured every 3 to 4 days, at approximately 80% confluency. HeLaS3 cell line and derived clones were maintained in suspension culture in EX-CELL HeLa Serum-Free Medium (14591 C, Sigma-Aldrich) containing 6 mM L-glutamine, at 37 ºC in a 5 % CO_2 atmosphere under agitation at 125 rpm (25 mm orbital diameter). Cells were subcultured every 3 to 4 days at a cell concentration of 0.3×10^6 cell/mL. PDT was calculated by the equation: PDT (*h*) = ln (2)/μ where μ = (ln [cell concentration 2] – ln [cell concentration 1])/(time of measurement 2 (h)/time of measurement 1(h)).

Generation of *GLUL* edited cell lines

To test *GLUL* based selection system, *GLUL* gene edited cells were generated using CRISPR-Cas9. The insertion of the CRISPR-Cas9 protein and the sgRNA was performed by nucleofection, using Lonza 4D-Nucleofector®, using the SE Cell Line Kit L (LONV4XC-1012, Lonza). A total of 8×10^5 HeLaS3 cells were centrifuged (90 g, 10 min) and resuspended in 10 μL RNP solution (2 μg/μL Cas9-GFP (ALT-R S. p. Cas9-GFP V3; 10008161, IDT) and 24 nM sgRNA (5' - AAAUUCCACUCAGGCAACUC - 3') + 30 μL nucleofection solution. Cells were nucleofected with program DS-150 and seeded in 1 mL of DMEM + 10 % FBS + 4 mM L-glutamine. Five days after editing the *GLUL* gene, cells were seeded at a concentration of 1 cell/well in a 96 well-plate in DMEM + 10 % FBS + 4 mM L-glutamine. To guarantee clonality, the growth was followed by imaging the wells at a 4x amplification using the cell imaging multimode reader CytationTM 3 (BioTek), at days 0 (1 h after plating), 3 and 10 after plating.

CRISPR-Cas9 editing efficiency on *GLUL* gene

CRISPR-Cas9 editing efficiency assay was performed based on the T7 Endonuclease I-based mutation detection method with the EnGen® Mutation Detection Kit (NEB #E3321) following manufacturer´s protocol. Fragments were run in a 4-20 % polyacrylamide TBE gel (EC62255BOX, Invitrogen) in a 0.5× TBE buffer (Novex). The percentage of gene modification was estimated by the ratio between the edited and wild-type band, previously normalized by respective molecular weight.

Western Blot

Cell pellets for western blot were homogenized in lysis buffer consisting of 4x NuPAGE™ LDS Sample Buffer (NP0007, Invitrogen) and 10x NuPAGE™ Sample Reducing Agent

(NP0004, Invitrogen) diluted in molecular grade water and incubated at 70 ºC for 10 min. Samples were run in a 4-12 % polyacrylamide gel (NP0321BOX, Invitrogen). Gel was transferred to a nitrocellulose membrane. The membrane was incubated with anti-GLUL (1:5000, ab7359, abcam) and anti-actin (1:5000, A5441, Sigma) antibodies. The secondary antibodies used were Anti-rabbit, (NA9341, Cytiva), for GLUL detection, and Anti-mouse (NA931-1ML, Cytiva), for β-actin detection, diluted 1:50000. Membranes were imaged using iBright (Invitrogen).

Digital droplet PCR quantification of copy number

The ddPCR reaction was performed with ddPCR Supermix for Probes (No dUTP) (1863024, Bio-Rad), primers (900 nM final concentration) for the albumin gene (Fw: 5'-GCTGTGAAAAACCTCTGTTGG-3'; Rv: 5'-GACATCCTTTGCCTCAGCAT-3') and the BGH poly A motif (Fw: 5'-TCTAGTTGCCAGCCATCTGTTGT-3'; 5'-TGGGAGTGGCACCTTCCA–3'), as a proxy plasmid insertion, and probes (250 nM final concentration) for the same sequences (5'-/5-HEX/AGTGGAAAA/ZEN/TGATGAGATGCCTGCT/3/AbkFQ/-3' and 5'-/56-FAM/ TCCCCCGTG/ZEN/CCTTCCTTGACC/3/AbkFQ/-3', respectively). ddPCR was performed using the QX200 AutoDG Droplet Digital PCR System (Bio-rad).

Establishment of rAAV producers cell lines

HeLaS3 cells with *GLUL* gene knock-out were nucleofected with the rAAV-*GLUL* plasmid, as previously published[7]. Cells were initially cultured for 3 days in EX-CELL HeLa medium supplemented with glutamine. Following this period, the medium was replaced with EX-CELL HeLa serum-free medium lacking glutamine. Cells were seeded at a density of 0.5 × 10□ cells/mL and subcultured every 3–4 days by complete medium exchange. After three weeks selected cells were tested for rAAV production as described below and seeded at 3 cell/well in serum-free medium with a single-cell growth supplement to generate single-cell clones as described previously [9]. Single-cell clones were further tested for rAAV production as described previously [7].

rAAV production and titration

To test rAAV production in suspension, cells were seeded at 0.5×10^6 cell/mL in serum-free medium diluted in DMEM, with supplementation and infected with wtAd5 at an MOI of 1. Cells were maintained for 3 days at 37 ºC and in a 5 % CO_2 atmosphere under agitation at 125 rpm, in 25 mm orbital diameter. Cells were harvested for rAAV quantification according to previously published protocol[7].

rAAV5 Purification and Full-to-Empty Capsid Quantification

Producer cells were harvested by centrifugation at 300 × *g* for 5 min and resuspended in 1 mL of lysis buffer (50 mM Tris-HCl, pH 8.0; 20 mM $MgCl_2$; 1% Tween-20). Benzonase was added at 150 U/mL, and the suspension was incubated for 1.5 h at 37□°C to degrade nucleic acids. Subsequently, NaCl was added to a final concentration of 200 mM, followed by a 15 min incubation at 37□°C. The lysate was clarified by centrifugation at 4,000 × *g* for 5 min and filtration through a 0.45 µm membrane.

Purification of rAAV5 particles was performed using PhyTip™ columns according to the manufacturer's protocol, with minor adjustments. Columns were equilibrated with 50 mM Tris (pH 8.0), 350 mM NaCl, and 0.001% Pluronic F-68, followed by six capture cycles of the sample. Washing was carried out in two steps: first with 50 mM Tris (pH 8.0), 1 M NaCl, and 0.001% Pluronic, and then with 50 mM Tris (pH 8.0) containing 0.001% Pluronic. Elution was performed in four cycles using 50 mM citric acid (pH 2.5) with 0.001% Pluronic. The eluate (approximately 60 µL) was immediately neutralized with Tris buffer (pH 9.0) at a 1:5 dilution. The ratio of full to empty capsids was determined by mass photometry using a SamuxMP instrument (Refeyn).

rAAV Infectious Units Quantification

rAAV infectious titer was determined as described in Fernandes et al 2025 [22] with some modifications. HeLa RC32 were plated in 96 well plates at a cell concentration of 15 000 cells/well in DMEM + 10% FBS + 4 mM L Glutamine and incubated overnight at 37 ºC in a 5% CO_2 atmosphere. Cells were infected at an rAAV MOI of $6.67x10^4$ vg/cell in DMEM + 1% FBS + 4 mM L Glutamine containing $3.20x10^8$ wtAd5 DNAse resistant genomes/mL. Cells were infected by total medium exchange and incubated for 2 h. Subsequently, the culture medium was diluted 1:2 with DMEM + 10% FBS + 4 mM L Glutamine. Images were acquired at 48 h post-infection with 10x amplification using MICA microscope (Leica).

Acknowledgements

The author(s) gratefully acknowledge the members of the laboratory for their insightful discussions and constructive feedback throughout the development of this work.

Author contributions

M.A writing – original draft, investigation, methodology, visualization, and formal analysis. F.M., investigation, methodology, visualization, and formal analysis. I.R.S investigation, methodology, and formal analysis. P.M.A, supervision and funding acquisition P.G.A. supervision, project supervision, project administration, funding

365 acquisition. J.M.E., writing – original draft, project conceptualization, supervision, project
366 supervision, investigation, funding acquisition. All authors: writing – review & editing.

367 Competing interests

368 The authors don't have competing interests.

369 Funding

370 This work was supported by the Research Unit UID/04462: iNOVA4Health – Programme
371 in Translational Medicine, financially supported by Fundação para a Ciência e
372 Tecnologia / Ministério da Educação, Ciência e Inovação
373 (PTDC_BTM_ORG_1383_2020), the Associate Laboratory LS4FUTURE
374 (LA/P/0087/2020) and the AAVscreen iBETXplore Grant. J.M.E is funded by Stimulus of
375 Scientific Employment, Individual Support program (2020. 01216.CEECIND) and F.M.
376 by PhD fellowship 2022.11494.BD from FCT. I.R.S. appreciate support by the FWF PhD
377 Program Grant 10.55776/W1224 "Biotechnology of Proteins – BioTop".

378 Data availability

379 All research data and methods presented in the main and supplementary figures are
380 available from the lead contact upon reasonable request. Correspondence and requests
381 for materials should be directed to J.M.E. (jose.escandell@ibet.pt).

382 Figure Legends

383 **Figure 1. Generation and validation of *GLUL*$^{-/-}$ HeLaS3 cell lines.**
384 (A) Schematic representation of the *GLUL* gene structure, showing three transcript
385 variants with exons represented as boxes and coding sequences highlighted in yellow.
386 Exon 5, where the protein catalytic site is located, is also highlighted in orange. (B) T7
387 endonuclease I assay of PCR-amplified genomic DNA from nucleofected cells. Original
388 gel is presented in Supplementary Figure 7. (C) Phase-contrast microscopy images of
389 *GLUL*$^{-/-}$ clones GKO1, GKO2, and GKO3 at Day 0, Day 3, and Day 10 post single-cell
390 seeding. White arrows indicate clonal outgrowth. (D) Western blot analysis of GLUL
391 protein expression in parental HeLaS3 (*GLUL*$^{+/+}$) and *GLUL*$^{-/-}$ clones. β-actin was used
392 as a loading control. Original blots are presented in Supplementary Figure 8.

393 **Figure 2. Viability of HeLaS3 wild-type and *GLUL*$^{-/-}$ clones under Gln-supplemented**
394 **and Gln-depleted conditions.**
395 Cells were cultured in standard conditions in serum-containing medium supplemented

with Gln (A) or depleted of Gln (B). Five cell viability measurements were taken by Trypan blue exclusion method over a 9 day period.

Figure 3. Establishment and characterization of rAAV producer clones using *GLUL*-based selection in suspension-adapted HeLaS3 cells.

(A) Schematic overview of the streamlined 2-month workflow for rAAV producer cell line generation. The process includes plasmid transfection, 3-week selection in Gln-depleted suspension culture, 4-week single-cell cloning, and expansion of selected producer clones. (B) Cell viability and viable cell density (VCD) of HeLaS3 cells non-transfected (in black) or transfected with the rAAV-*GLUL* producer plasmid (in pink) cultured in Gln-depleted EX-CELL medium over time. The selected pool underwent single-cell cloning, and 120 wells with clonal outgrowth were screened for productivity. rAAV5 vector genome titers (vg/mL) (C) and qP (D) were measured in culture cell lysates of selected clones by qPCR.

Figure 4. Characterization of rAAV5 production and GLUL expression in HeLaS3-derived cell lines.

(A) Quantification of rAAV5 vector genome (vg) titers expressed as vg/mL for Clone 1, Clone 2, and Clone 3 across different amplification stages: primary screen, secondary screen (static culture), and suspension culture production. Data shown as mean ± SD (n=2) is presented for suspension culture conditions.

(B) Western blot analysis of GLUL protein levels with β-actin as loading control across HeLaS3 *GLUL*$^{-/-}$, transfected Pool, Clone 1, Clone 2, and Clone 3. Original blots are presented in Supplementary Figure 9. (C) Digital Droplet PCR analysis of rAAV5 plasmid copy number per cell for the same cell lines. Data shown as mean ± SD (n=2). (D) Mass photometry analysis of rAAV5 particles purified from Clone 1 production, showing empty capsids (~3.7 MDa) and full capsids (~4.7 MDa).

Figure 5. Optimization of rAAV5 production in HeLaS3-derived cell lines.

(A) Population doubling time (PDT) and viability of rAAV5 producer Clone 1 grown in the presence (black square) or absence (pink circle) of Gln in growth media. Cells were cultured in standard serum-free conditions and subcultured every 3-4 days. (B) rAAV5 vector genome titers (vg/mL; black bars) and Cell specific production yield (qP, vg/cell; pink bars) measured in culture cell lysates by qPCR of Clone 1 with production media either supplemented or depleted of Gln. Data shown as mean ± SD (n=4). Statistical analysis was performed using unpaired t-test with Welch's correction (*: $p < 0.05$; ***: $p < 0.001$). (C) Representation of ammonia (NH_3) concentration (mM) up to 66 h post wtAd5 infection, either in Gln-supplemented medium (black circles) or Gln-depleted (pink squares). Data shown as mean ± SD (n=4). (D) Gln and NH_3 metabolic rates (mM/10^6

cells h^{-1}) with production media either supplemented (black bars) or depleted (pink bars) in Gln. Data shown as mean ± SD (n=3). Statistical analysis was performed using unpaired t-test with Welch's correction (*: $p < 0.05$; ***: $p < 0.001$).

References

1. Zwi-Dantsis, L., Mohamed, S., Massaro, G. & Moeendarbary, E. Adeno-Associated Virus Vectors: Principles, Practices, and Prospects in Gene Therapy. *Viruses 2025, Vol. 17, Page 239* **17**, 239 (2025).

2. Liu, Z. *et al.* The clinical safety landscape for ocular AAV gene therapies: A systematic review and meta-analysis. *iScience* **28**, 112265 (2025).

3. Reid, C. A., Hörer, M. & Mandegar, M. A. Advancing AAV production with high-throughput screening and transcriptomics. *Cell Gene Ther Insights* **10**, 821–840 (2024).

4. Merten, O.-W. Development of Stable Packaging and Producer Cell Lines for the Production of AAV Vectors. *Microorganisms* **12**, 384 (2024).

5. Escandell, J. M. *et al.* Leveraging rAAV bioprocess understanding and next generation bioanalytics development. *Curr Opin Biotechnol* **74**, 271–277 (2022).

6. Clark, K. R., Voulgaropoulou, F., Fraley, D. M. & Johnson, P. R. Cell lines for the production of recombinant adeno-associated virus. *Hum Gene Ther* **6**, 1329–1341 (1995).

7. Escandell, J. *et al.* Towards a scalable bioprocess for rAAV production using a HeLa stable cell line. *Biotechnol Bioeng* **120**, 2578–2587 (2023).

8. Martin, J. *et al.* Generation and characterization of adeno-associated virus producer cell lines for research and preclinical vector production. *Hum Gene Ther Methods* **24**, 253–269 (2013).

9. Escandell, J. M. *et al.* Development of a Serum-Free Producer Cell Line Generation Process for Scalable and Efficient rAAV Production for gene therapy applications. *bioRxiv* 2025.10.02.679972 (2025) doi:10.1101/2025.10.02.679972.

10. Yu, D. Y., Lee, S. Y. & Lee, G. M. Glutamine synthetase gene knockout-human embryonic kidney 293E cells for stable production of monoclonal antibodies. *Biotechnol Bioeng* **115**, 1367–1372 (2018).

11. Chin, C. L. *et al.* A human expression system based on HEK293 for the stable production of recombinant erythropoietin. *Sci Rep* **9**, (2019).

12. Fan, L., Frye, C. C. & Racher, A. J. The use of glutamine synthetase as a selection marker: recent advances in Chinese hamster ovary cell line generation processes. *Pharm Bioprocess* **1**, 487–502 (2013).

13. Srivastava, A., Mallela, K. M. G., Deorkar, N. & Brophy, G. Manufacturing Challenges and Rational Formulation Development for AAV Viral Vectors. *J Pharm Sci* **110**, 2609–2624 (2021).

14. Xue, W. *et al.* Adeno-associated virus perfusion enhanced expression: A commercially scalable, high titer, high quality producer cell line process. *Mol Ther Methods Clin Dev* **32**, 101266 (2024).

15. Prasad, A. *et al.* Low-dose exposure to phytosynthesized gold nanoparticles combined with glutamine deprivation enhances cell death in the cancer cell line HeLa *via* oxidative stress-mediated mitochondrial dysfunction and G0/G1 cell cycle arrest. *Nanoscale* **14**, 10399–10417 (2022).

16. Reitzer, L. J., Wice, B. M. & Kennell, D. Evidence that glutamine, not sugar, is the major energy source for cultured HeLa cells. *J Biol Chem* **254**, 2669–76 (1979).

17. Srila, W. *et al.* Glutamine synthetase (GS) knockout (KO) using CRISPR/Cpf1 diversely enhances selection efficiency of CHO cells expressing therapeutic antibodies. *Sci Rep* **13**, (2023).

18. Fu, Q., Polanco, A., Lee, Y. S. & Yoon, S. Critical challenges and advances in recombinant adeno-associated virus (rAAV) biomanufacturing. *Biotechnol Bioeng* **120**, 2601–2621 (2023).

19. Destro, F. *et al.* The state of technological advancement to address challenges in the manufacture of rAAV gene therapies. *Biotechnology Advances* vol. 76 Preprint at https://doi.org/10.1016/j.biotechadv.2024.108433 (2024).

20. Lorek, J. K., Isaksson, M. & Nilsson, B. Chromatography in Downstream Processing of Recombinant Adeno-Associated Viruses: A Review of Current and Future Practises. *Biotechnology and Bioengineering* vol. 122 1067–1086 Preprint at https://doi.org/10.1002/bit.28932 (2025).

21. FDA. *Manufacturing Changes and Comparability for Human Cellular and Gene Therapy Products; Draft Guidance for Industry*. http://www.regulations.gov. (2023).

22. Fernandes, S., Guerra, J., Ferreira, M. V. & Coroadinha, A. S. Deciphering Key Adenoviral Elements in the Production of Recombinant Adeno-Associated Virus Vectors. *Hum Gene Ther* **36**, (2025).

A)

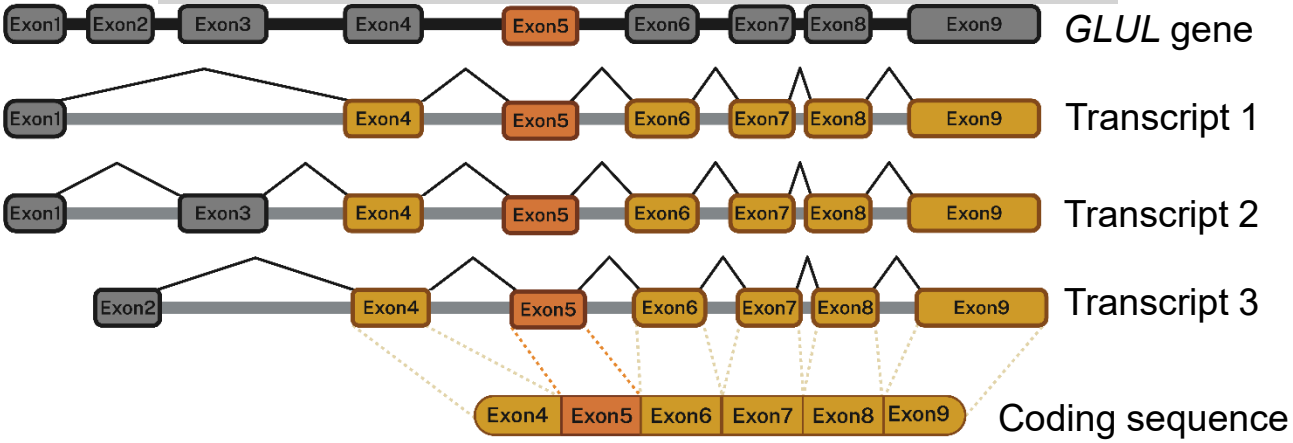

B)

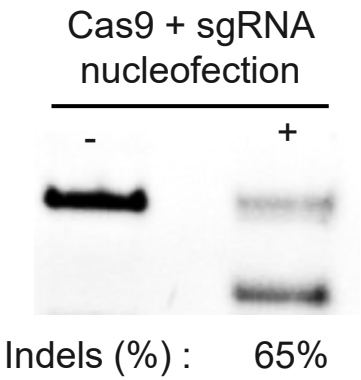

C)

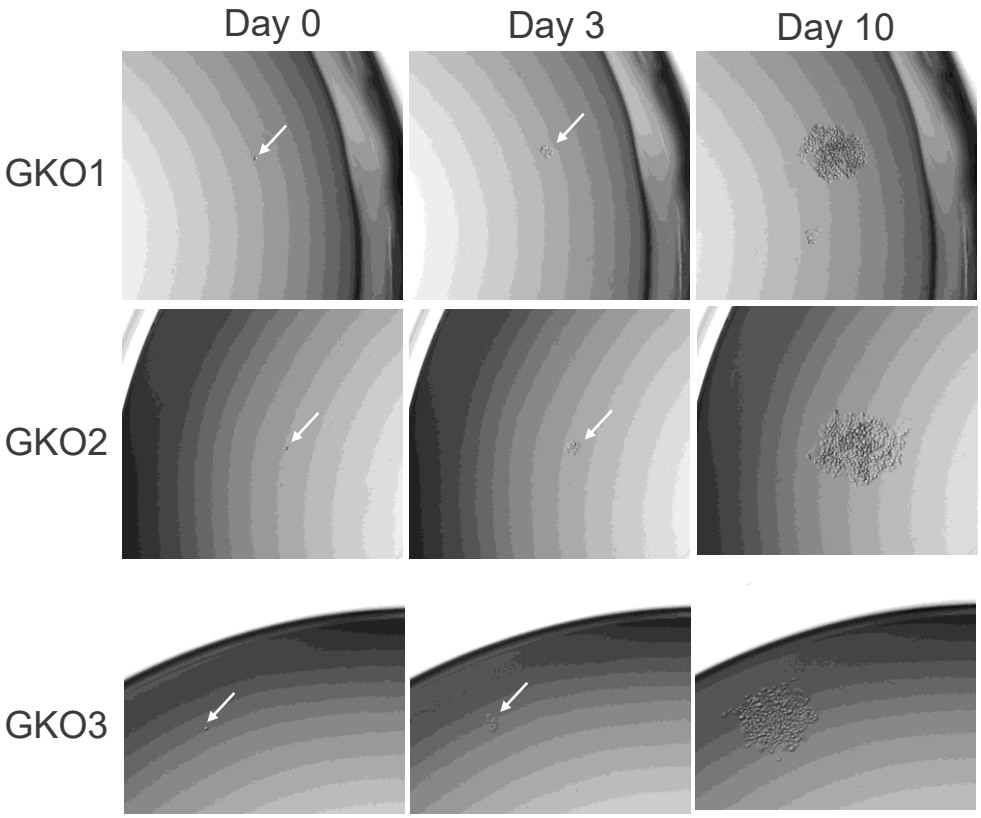

D)

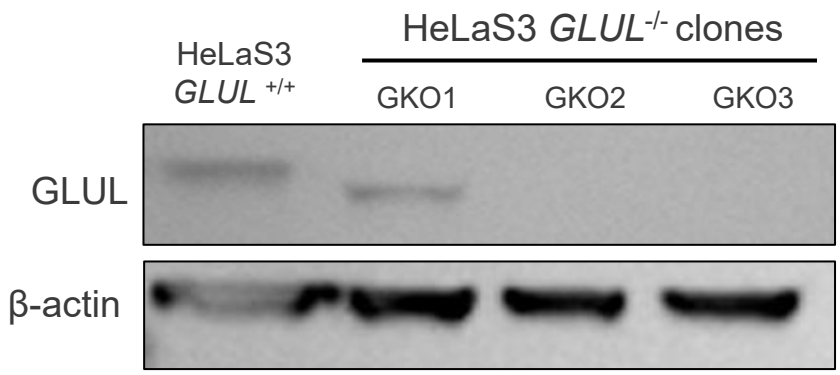

Figure 1

A)

Glutamine Supplemented medium

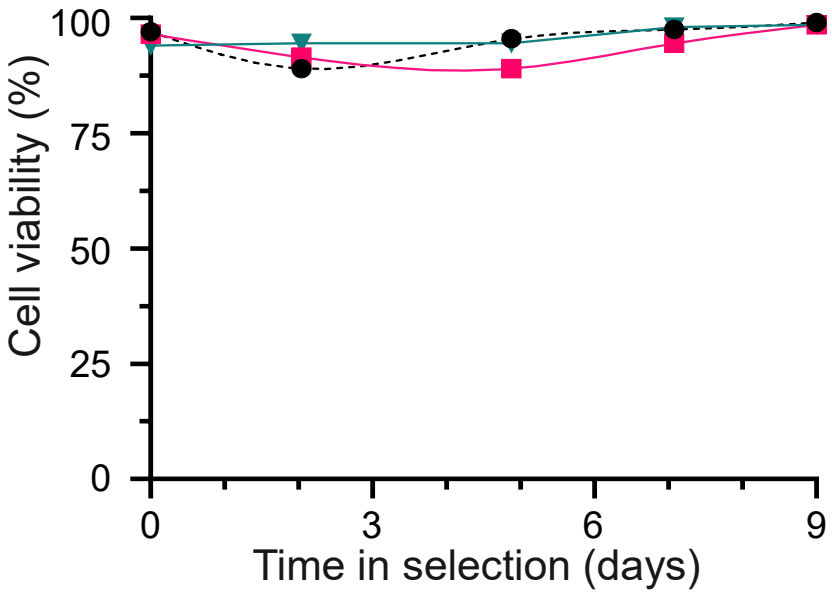

B)

Glutamine depleted conditions

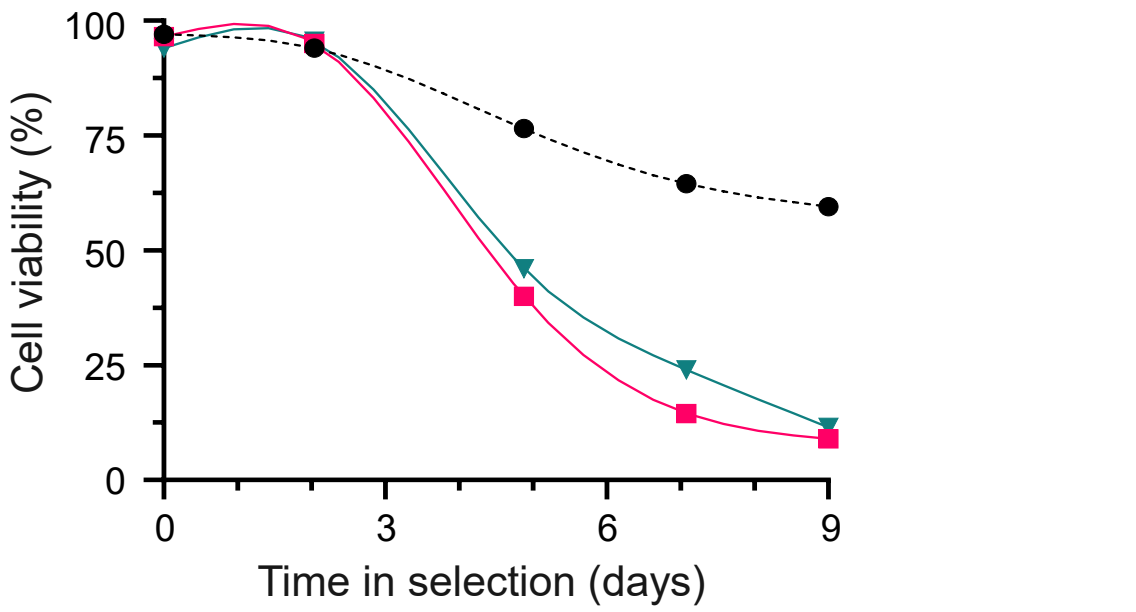

Figure 2

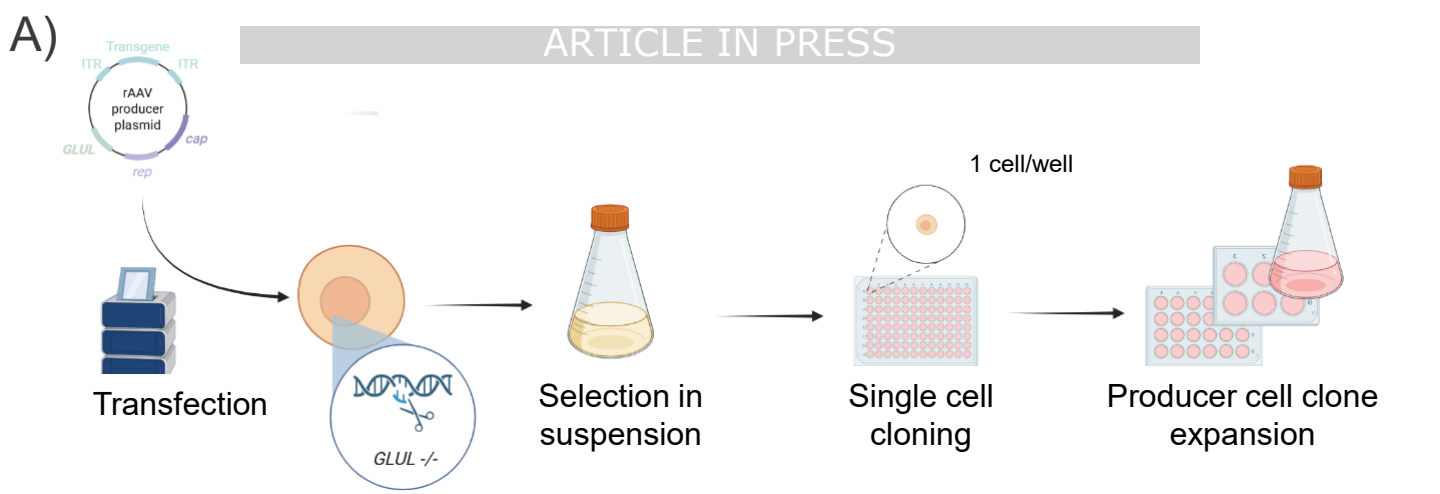
A)
Transgene
ITR
ITR
rAAV producer plasmid
GLUL
cap
rep
Transfection
GLUL -/-
Selection in suspension
1 cell/well
Single cell cloning
Producer cell clone expansion

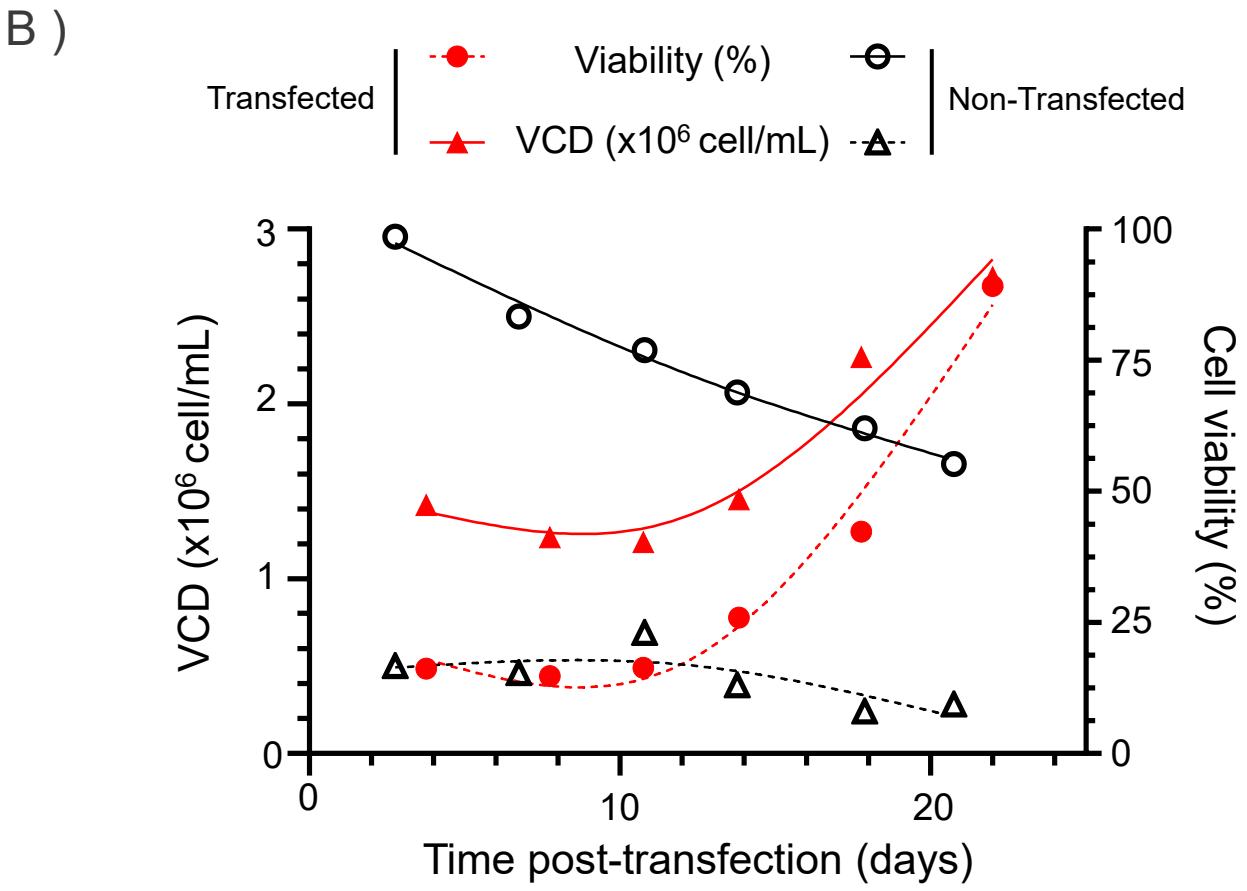
B)
Transfected
Viability (%)
VCD (x10⁶ cell/mL)
Non-Transfected
VCD (x10⁶ cell/mL)
Cell viability (%)
Time post-transfection (days)
0
1
2
3
0
10
20
0
25
50
75
100

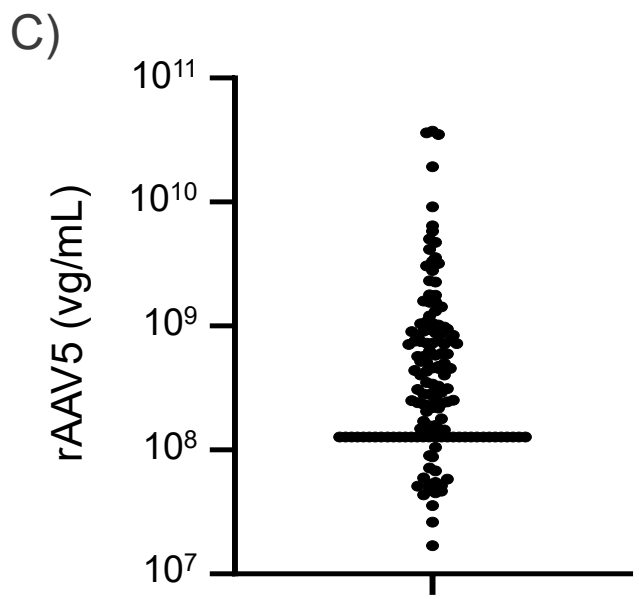
C)
rAAV5 (vg/mL)
10¹¹
10¹⁰
10⁹
10⁸
10⁷

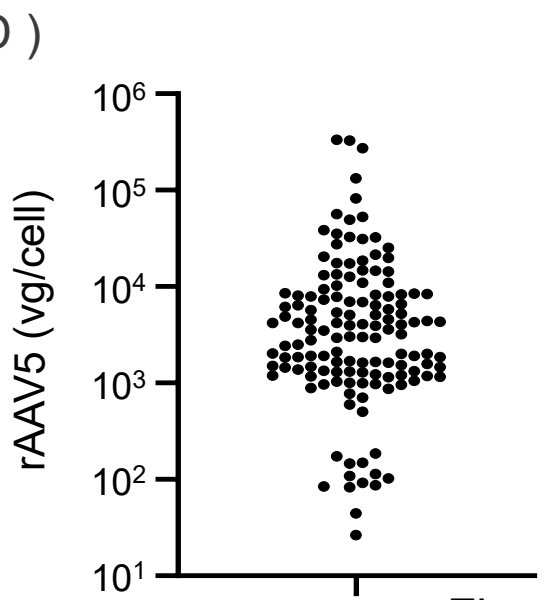
D)
rAAV5 (vg/cell)
10⁶
10⁵
10⁴
10³
10²
10¹

Figure 3

A)

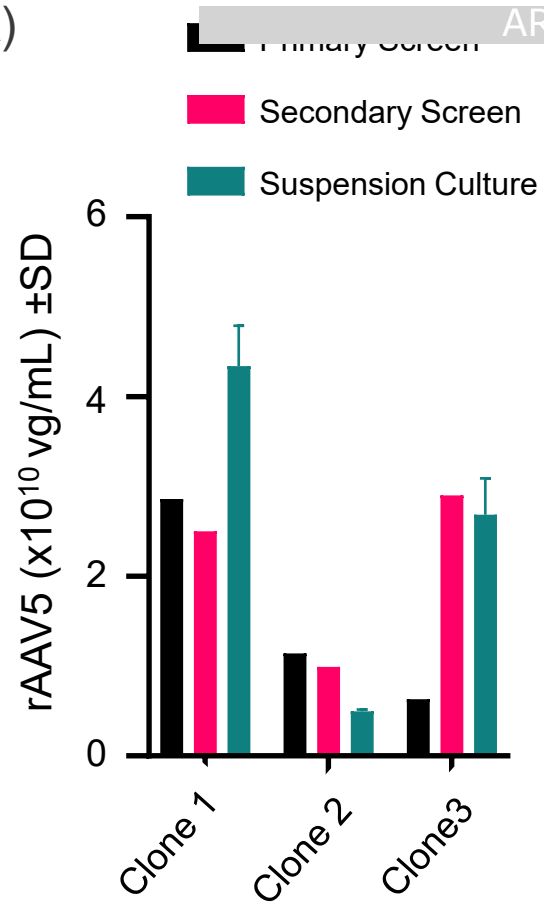

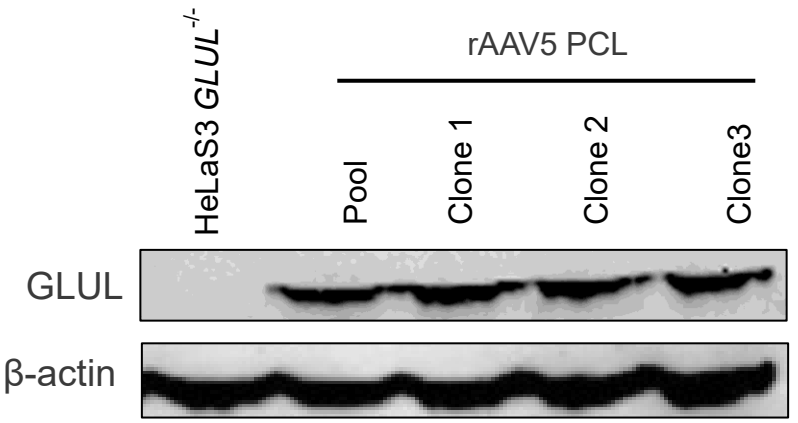

C)

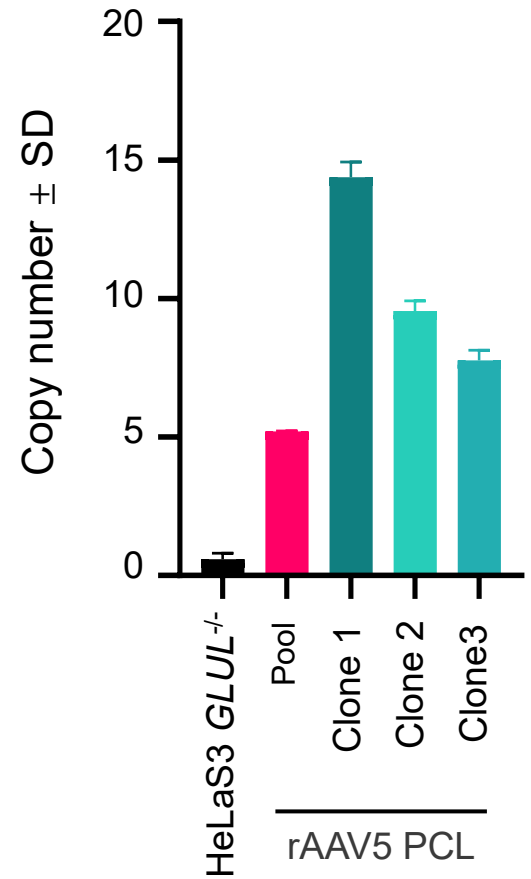

D)

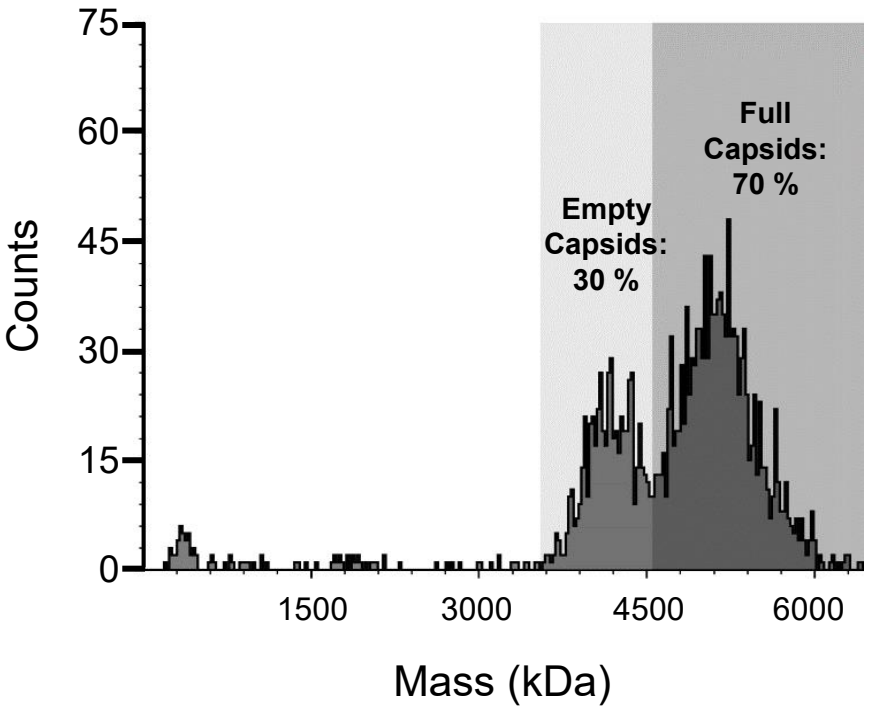

Figure 4

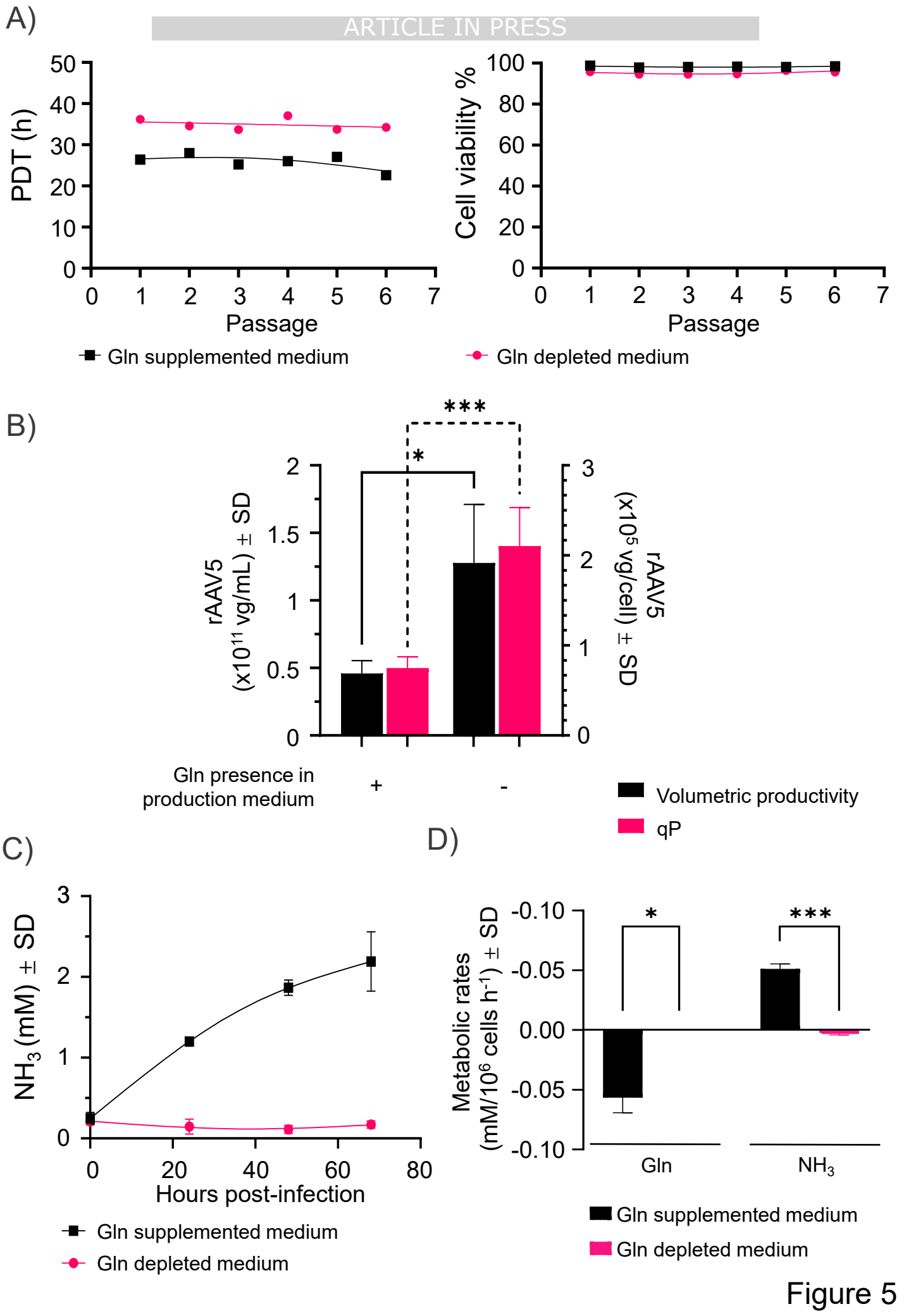

Figure 5